J. Numer. Math., Vol. 0, No. 0, pp. 1–20 (2004)
 Prepared using jnm.sty [Version: 02.02.2002 v1.2]

Convergence of Mimetic Finite Difference Discretizations of the Diffusion Equation

M. BERNDT*, K. LIPNIKOV†, D. MOULTON*, and M. SHASHKOV*

Received 20 November, 2001 *Communicated by Yu. A. Kuznetsov*
Received in revised form 1 December, 2001

Abstract — The main goal of this paper is to establish the convergence of mimetic discretizations of the first-order system that describes linear diffusion. Specifically, mimetic discretizations based on the support-operators methodology (SO) have been applied successfully in a number of application areas, including diffusion and electromagnetics. These discretizations have demonstrated excellent robustness, however, a rigorous convergence proof has been lacking. In this research, we prove convergence of the SO discretization for linear diffusion by first developing a connection of this mimetic discretization with Mixed Finite Element (MFE) methods. This connection facilitates the application of existing tools and error estimates from the finite element literature to establish convergence for the SO discretization. The convergence properties of the SO discretization are verified with numerical examples.

Keywords: mimetic discretizations, mixed finite elements, error estimates

1. INTRODUCTION

In many applications, the mathematical model is formulated initially as a system of first-order partial differential equations (PDE's), with each equation having a natural connection to physical aspects of the problem (e.g., mass conservation). Thus, the increasing demand for accurate and robust numerical simulations has generated considerable interest in discretizations of this first-order form. One such methodology, the mimetic finite difference technique based on support-operators (SO), has been applied successfully to several applications including diffusion [12,6,8,7], electromagnetics [5], and gas dynamics [3]. In particular, the numerical convergence of the SO discretization has been demonstrated in the presence of grid distortions and severe jumps in coefficients. However, a formal convergence proof of the SO discretization has been lacking, even for smooth coefficients on smooth grids.

The main goal of this work is to derive rigorous error estimates for the SO

*Los Alamos National Laboratory, Theoretical Division, Mail Stop B284, Los Alamos, NM, 87545. Email: berndt@lanl.gov, moulton@lanl.gov, shashkov@lanl.gov. Sponsored by the Department of Energy, under contract W-7405-ENG-36.

†Department of Mathematics, University of Houston, Houston, TX, 77204, Email: lipnikov@math.uh.edu. Supported by the Los Alamos Computer Science Institute (LACSI).

discretization of the stationary linear diffusion equation. Specifically, we focus on the linear elliptic boundary value problem

$$\operatorname{div} \mathbf{w} = f, \tag{1.1a}$$

$$\mathbf{w} = -K \operatorname{grad} p, \tag{1.1b}$$

given in a bounded polygonal convex domain Ω and subject to homogeneous Dirichlet boundary conditions (i.e., $p = 0$ on Ω). Here, the unknowns are the scalar function p (e.g., pressure or temperature), and the vector function $\mathbf{w}$ (e.g., velocity or flux). Further, we assume that both the source f and the symmetric positive definite diffusion tensor K, are sufficiently smooth functions given on Ω. In this form, it is readily apparent that conservation of the scalar is described by (1.1a) and the definition of the flux is given in (1.1b). Moreover, the symmetric positive definite nature of the underlying elliptic problem is apparent from the fact that the negative divergence is self adjoint to the gradient. The mimetic approach of the SO discretization is based on preserving these properties on a discrete level through the use of integral identities (e.g., Green's Theorem) and the definition of corresponding discrete inner products. In this manner, the SO discretization forms a weak specification of the diffusion equation that is connected to the mixed finite element (MFE) formulation.

In Section 2, we describe the basic error estimates for MFE methods on triangular and quadrilateral grids. Using an appropriate quadrature rule to compute the scalar product of two fluxes, we obtain an alternate proof of the error estimates for the lowest order modified Raviart-Thomas (RT) finite elements on quadrilateral grids [11,13]. We note that error estimates for RT finite elements of arbitrary order on quadrilateral grids were proved by Wang and Mathew [15]. However, on quadrilateral grids, the connection of SO discretization and MFE methods through quadrature is best made with the lowest order modified RT basis [11,13].

Thus, our error analysis proceeds by formalizing the relationship between the SO discretization and the lowest order RT MFE methods [10]. Then, we show that the error in the SO discretization can be estimated via Strang's first lemma (see, e.g., [4]). Specifically, the discretization error of the SO discretization can be bounded from above by a sum of two errors: The best approximation error for the RT finite elements, and a consistency error introduced by the quadrature. Our main result is that the consistency error is less than, or of the same order of magnitude as, the best approximation error. Thus, the SO discretization is at least of the same order of accuracy as the lowest order RT finite element method. In Section 3, we derive optimal error estimates for the SO discretization on both triangular and quadrilateral grids. The validity of the theoretical results is demonstrated with numerical experiments in Section 4. Finally, conclusions are presented in Section 5.

2. MIXED METHODS

In this section, we briefly review the major error estimates for mixed methods for the Dirichlet problem (1.1). Applying Strang's first lemma [4], we confirm error estimates for the lowest order Raviart-Thomas finite elements on quadrilaterals which were first derived in [13]. Contrary to the approach described in [13], our analysis is based on considering a discrete system resulting from the RT finite elements as an application of special quadrature rules for integrals involving the modified RT finite elements. Later, we shall use similar approach to derive error estimates for the support-operators method.

Throughout this paper, we shall use notations $\|\cdot\|_{1,D}$, $\|\cdot\|_{\mathrm{div},D}$ and $\|\cdot\|_D$ for the norms on the Hilbert spaces $H^1(D)$, $H(\mathrm{div};D)$ and $L_2(D)$, respectively, for some set $D \subset \Omega$. In addition, we denote by $(\cdot,\cdot)_D$ the inner product on D of either scalar or vector functions, and by $|\cdot|_{1,D}$ the seminorm on $H^1(D)$. Let $X \equiv H(\mathrm{div};\Omega)$, $Q \equiv L_2(\Omega)$, and $(\cdot,\cdot) \equiv (\cdot,\cdot)_\Omega$.

Introducing the flux variable $\mathbf{v} = -K\nabla p$, we consider a dual mixed variational formulation of (1.1) given by characterizing the pair $(\mathbf{v}, p) \in X \times Q$ as the solution of

$$\begin{aligned} (K^{-1}\mathbf{v}, \mathbf{w}) - (p, \operatorname{div}\mathbf{w}) &= 0, \\ (q, \operatorname{div}\mathbf{v}) &= (f, q), \qquad \forall(\mathbf{w}, q) \in X \times Q. \end{aligned} \tag{2.1}$$

For the discretization of (2.1), denote by $\mathscr{T}_h = \{e_1, e_2, \dots, e_M\}$ a *shape regular* partition (see [1], p. 113, Remark 2.2) of $\bar{\Omega}$ into triangular or convex quadrilateral elements of diameter not greater than h, $0 < h < 1$. For two examples of shape regular grids, see Figure 2. Given finite dimensional subspaces X_h and Q_h of X and Q, respectively, we define the discrete problem: find $(\mathbf{v}^h, p^h) \in X_h \times Q_h$ satisfying

$$\begin{aligned} (K^{-1}\mathbf{v}^h, \mathbf{w}^h)_h - (p^h, \operatorname{div}\mathbf{w}^h) &= 0, \\ (q^h, \operatorname{div}\mathbf{v}^h) &= (f, q^h), \qquad \forall(\mathbf{w}^h, q^h) \in X_h \times Q_h, \end{aligned} \tag{2.2}$$

where $(\cdot,\cdot)_h$ is continuous bilinear form corresponding to an application of a quadrature rule for computing $(\cdot,\cdot)$. A few suitable choices for the pair of finite element spaces X_h and Q_h were proposed and analyzed in [10]. When the mesh $\mathscr{T}_h$ consists of convex quadrilaterals, we shall use the modified RT finite element spaces proposed and studied in [13]. Denote by P_0 the space of constant functions. For the triangular partition $\mathscr{T}_h$ the lowest order RT finite elements spaces are

$$\begin{aligned} X_h = \{\mathbf{w} \in L_2(\Omega)^2 :\ & \mathbf{w}|_e \in P_0(e) \times P_0(e) + P_0(e)\mathbf{r} \quad \forall e \in \mathscr{T}_h, \\ & \mathbf{w}|_{e_1} \cdot \mathbf{n}_1 + \mathbf{w}|_{e_2} \cdot \mathbf{n}_2 = 0 \quad \forall \gamma = e_1 \cap e_2, \quad e_1, e_2 \in \mathscr{T}_h\}, \\ Q_h = \{q \in L_2(\Omega) :\ & q|_e \in P_0(e) \quad \forall e \in \mathscr{T}_h\}, \end{aligned} \tag{2.3}$$

where $\mathbf{n}_1$ is a unit vector normal to edge γ and $\mathbf{n}_2 = -\mathbf{n}_1$. In other words, X_h is the space of piecewise linear vector functions with normal component continuous across each mesh edge, and Q_h is the space of piecewise constant functions.

If $\mathscr{T}_h$ consists of convex quadrilaterals, then some additional notation is necessary. For any $e \in \mathscr{T}_h$ there exists a bijection $\mathbf{F}_e : \hat{e} \to e$, where $\hat{e}$ is the reference unit square having vertices $(0,0)^t$, $(1,0)^t$, $(1,1)^t$ and $(0,1)^t$. Denote by $\mathbf{r}_i = (x_i, y_i)^t$, $i = 1,2,3,4$, the four vertices of element e counted counter-clockwise (see Fig.1). Then $\mathbf{F}_e$ is the bilinear mapping given by

$$\mathbf{F}_e(\hat{\mathbf{r}}) = \mathbf{r}_1(1-\hat{x})(1-\hat{y}) + \mathbf{r}_2\hat{x}(1-\hat{y}) + \mathbf{r}_3\hat{x}\hat{y} + \mathbf{r}_4(1-\hat{x})\hat{y}. \tag{2.4}$$

Note that the Jacobi matrix $\mathscr{J}_e$ and its Jacobian J_e are linear functions of the coordinates $\hat{x}$ and $\hat{y}$. Straightforward computations yield

$$\mathscr{J}_e = [(1-\hat{y})\,\mathbf{r}_{21} + \hat{y}\,\mathbf{r}_{34},\ (1-\hat{x})\,\mathbf{r}_{41} + \hat{x}\,\mathbf{r}_{32}], \tag{2.5}$$

and

$$J_e = 2|T_{124}| + 2(|T_{123}| - |T_{124}|)\hat{x} + 2(|T_{134}| - |T_{124}|)\hat{y}, \tag{2.6}$$

where $\mathbf{r}_{ij} = \mathbf{r}_i - \mathbf{r}_j$ and $|T_{ijk}|$ is the area of the triangle with vertices $\mathbf{r}_i$, $\mathbf{r}_j$ and $\mathbf{r}_k$. Since e is a convex element, the Jacobian J_e is always positive, $J_e > 0$. In the sequel, we shall omit the subscript e whenever it is not confusing.

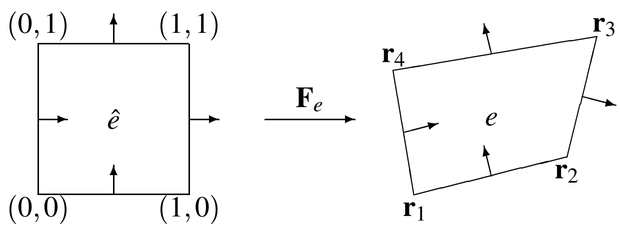

Figure 1. Bilinear mapping and orientation of normal vectors.

For partitions consisting of convex quadrilaterals, the lowest order RT finite element spaces are defined through Piola's transformation (the change of variables for vector functions):

$$\mathbf{F}_e^{-1} \circ \frac{1}{J_e}\mathscr{J}_e:\ L_2(\hat{e}) \to L_2(e), \qquad \forall e \in \mathscr{T}_h.$$

Two properties of Piola's transformation will be important for our analysis. Denote by $\hat{\mathbf{w}}$ a function defined on the reference element $\hat{e}$ and related to $\mathbf{w}^h$ defined on e via Piola's transformation, i.e., $\mathbf{w}^h = \mathbf{F}_e^{-1} \circ J_e^{-1}\mathscr{J}_e\hat{\mathbf{w}}$. Then

$$J_e \mathrm{div}\,\mathbf{w}^h = \hat{\mathrm{div}}\,\hat{\mathbf{w}}, \qquad \text{and} \qquad l_i\,\mathbf{w}^h \cdot \mathbf{n}_{ei} = \hat{\mathbf{w}} \cdot \hat{\mathbf{n}}_i, \quad i = 1, \ldots, 4,$$

where $\mathbf{n}_{ei}$ and $\hat{\mathbf{n}}_i$, $i = 1,2,3,4$, are unit vectors orthogonal to edges of e and $\hat{e}$, respectively, and l_i, $i = 1,2,3,4$, are lengths of four edges of element e counted counterclockwise starting with the edge $\mathbf{r}_1\mathbf{r}_2$ (see Fig. 1).

For the quadrilateral partition $\mathscr{T}_h$, the RT finite element spaces are given by

$$\begin{aligned} X_{1h} &= \{\mathbf{w} \in L_2(\Omega)^2:\ J_e\mathscr{J}_e^{-1}(\mathbf{w} \circ \mathbf{F}_e) \in P_{10}(\hat{e}) \times P_{01}(\hat{e}) \quad \forall e \in \mathscr{T}_h, & (2.7)\\ &\qquad \mathbf{w}|_{e_1} \cdot \mathbf{n}_1 + \mathbf{w}|_{e_2} \cdot \mathbf{n}_2 = 0 \quad \forall \gamma = e_1 \cap e_2, \quad e_1, e_2 \in \mathscr{T}_h\}, \\ Q_h &= \{q \in L_2(\Omega):\quad q|_e \in P_0(e) \quad \forall e \in \mathscr{T}_h\}, & (2.8) \end{aligned}$$

where P_{10} (or P_{01}) denotes a space of functions linear in the $\hat{x}$ (or $\hat{y}$) variable and constant in the other variable. Thomas [14] proposed (2.7), (2.8) without showing stability and approximation properties. Because the divergence of the discrete flux space is no longer a subspace of the discrete pressure space, a theoretical analysis of these properties is not trivial (see e.g. [13]). Therefore we shall use a modified discrete flux space proposed and analyzed in [13]. For each element e we define the vector function

$$\eta_e = \frac{1}{|e|}\begin{bmatrix} \alpha\hat{x}(\hat{x}-1) \\ \beta\hat{y}(\hat{y}-1) \end{bmatrix}, \tag{2.9}$$

where $\alpha = |T_{123}| - |T_{124}|$ and $\beta = |T_{134}| - |T_{124}|$. The modified RT basis functions are given by

$$\eta_{ei} = |l_i|\,(\varphi_i - \eta_e), \quad i = 1,4, \quad \text{and} \quad \eta_{ei} = |l_i|\,(\varphi_i + \eta_e), \quad i = 2,3, \tag{2.10}$$

where $\varphi_1 = (0,\, 1-\hat{y})^t$, $\varphi_2 = (\hat{x},\, 0)^t$, $\varphi_3 = (0,\, \hat{y})^t$ and $\varphi_4 = (1-\hat{x},\, 0)^t$ are the standard basis functions for $P_{10}(\hat{e}) \times P_{01}(\hat{e})$. Using the new basis functions, we define the modified discrete flux space by

$$\begin{aligned} X_{2h} = \{\mathbf{w} \in L_2(\Omega)^2 :\ & J_e \mathscr{J}_e^{-1}(\mathbf{w} \circ \mathbf{F}_e) \in span\{\eta_{e1}, \eta_{e2}, \eta_{e3}, \eta_{e4}\} \quad \forall e \in \mathscr{T}_h, \\ & \mathbf{w}|_{e_1} \cdot \mathbf{n}_1 + \mathbf{w}|_{e_2} \cdot \mathbf{n}_2 = 0 \quad \forall \gamma = e_1 \cap e_2, \quad e_1, e_2 \in \mathscr{T}_h\}. \end{aligned} \tag{2.11}$$

Note that for rectangular grids $\alpha = \beta = 0$ in (2.9) and two definitions (2.7) and (2.11) of the discrete flux space are equivalent.

Straightforward computations show that, for any $\mathbf{w}^h \in X_{2h}$, the divergence of $\mathbf{w}^h$ is a piecewise constant function,

$$(\operatorname{div} \mathbf{w}^h)|_e = \frac{1}{|e|}\left(w_{e2}|l_2| - w_{e4}|l_4| + w_{e3}|l_3| - w_{e1}|l_1|\right), \qquad \forall e \in \mathscr{T}_h, \tag{2.12}$$

where $w_{ei} = \mathbf{w}^h \cdot \mathbf{n}_{ei}$, $i = 1,2,3,4$.

2.1. Error estimates for the mixed FE method

Solvability of problem (2.2) is based on two stability conditions [2]. Denote by V_h the subspace of X_h that contains discrete divergent-free functions,

$$V_h = \{\mathbf{w}^h \in X_h :\ (\operatorname{div} \mathbf{w}^h, q^h) = 0 \quad \forall q^h \in Q_h\}. \tag{2.13}$$

We assume that there exist positive constants C_1, C_2, and C_3, such that the bilinear form $(\cdot, \cdot)_h$ is V_h-elliptic,

$$C_1\|\mathbf{w}^h\|^2_{\operatorname{div},\Omega} \leqslant (K^{-1}\mathbf{w}^h, \mathbf{w}^h)_h \leqslant C_2\|\mathbf{w}^h\|^2_{\operatorname{div},\Omega}, \qquad \forall \mathbf{w}^h \in V_h, \tag{2.14}$$

and the Ladyshenskaya-Babuška-Brezzi (LBB) condition holds, i.e.,

$$\sup_{\mathbf{w}^h \in X_h} \frac{(\operatorname{div} \mathbf{w}^h, q^h)}{\|\mathbf{w}^h\|_{\operatorname{div},\Omega}} \geqslant C_3\|q^h\|_\Omega, \qquad \forall q^h \in Q_h. \tag{2.15}$$

Solvability conditions for problem (2.1) are identical to (2.13)–(2.15), except functions $\mathbf{w} \in X$ and $q \in Q$ are used instead of $\mathbf{w}^h \in X_h$ and $q^h \in Q_h$, respectively, V_h is replaced by a subspace $V \subset X$ of divergent-free functions, and the quadrature is replaced by the exact scalar product.

Sufficient regularity for the solution of (2.1) is necessary to establish error estimates. Due to our previous assumptions, Ω is a convex polygonal domain and the entries of tensor K are sufficiently smooth, say in $C^1(\Omega)$. In addition, we require that $\mathbf{v} \in (H^1(\Omega))^2$ and $\operatorname{div}\mathbf{v} \in H^1(\Omega)$.

Theorem 2.1. *Suppose $\mathscr{T}_h$ is a shape regular partition of $\bar{\Omega}$. The pairs $(\mathbf{v}, p)$ and $(\mathbf{v}^h, p^h)$ are solutions of (2.1) and (2.2), respectively, with the discrete spaces X_h and Q_h given by (2.3) or (2.8), (2.11). Then*

$$\|\mathbf{v} - \mathbf{v}^h\|_{\mathrm{div},\Omega} \leqslant C \inf_{\mathbf{w}^h \in X_h} \left[\|\mathbf{v} - \mathbf{w}^h\|_{\mathrm{div},\Omega} + \Delta(\mathbf{w}^h) \right], \tag{2.16}$$

and

$$\|p - p^h\|_\Omega \leqslant C \left\{ \inf_{q^h \in Q_h} \|p - q^h\|_\Omega + \inf_{\mathbf{w}^h \in X_h} \left[\|\mathbf{v} - \mathbf{w}^h\|_\Omega + \Delta(\mathbf{w}^h) \right] \right\}, \tag{2.17}$$

where

$$\Delta(\mathbf{w}^h) = \sup_{\mathbf{u}^h \in X_h} \frac{|(K^{-1}\mathbf{w}^h, \mathbf{u}^h) - (K^{-1}\mathbf{w}^h, \mathbf{u}^h)_h|}{\|\mathbf{u}^h\|_{\mathrm{div},\Omega}} \tag{2.18}$$

is the consistency term and C is a positive constant independent of h.

Proof. The proof can be found in [2] for general spaces X_h and Q_h satisfying the stability conditions. The stability conditions for discrete spaces (2.3) and (2.8), (2.11) are proved in [2] and [13], respectively. □

Orthogonal projections play an important role in error estimates for mixed FE methods. Let $P_h\colon Q \to Q_h$ be the standard L_2 projection:

$$(q - P_h q, s^h) = 0, \qquad \forall s^h \in Q_h, \tag{2.19}$$

and $\Pi_h\colon (H^1(\Omega))^2 \to X_h$ be an extension of the Raviart-Thomas projection [13]:

$$(\operatorname{div}(\mathbf{w} - \Pi_h \mathbf{w}), s^h) = 0, \qquad \forall s^h \in Q_h. \tag{2.20}$$

Theorem 2.2. *Under assumptions of Theorem 2.1,*

$$\|\Pi_h \mathbf{v} - \mathbf{v}^h\|_\Omega \leqslant C\, |(K^{-1}\Pi_h \mathbf{v}, \Pi_h \mathbf{v} - \mathbf{v}^h)_h - (K^{-1}\mathbf{v}, \Pi_h \mathbf{v} - \mathbf{v}^h)|^{1/2}, \tag{2.21}$$

and

$$\|\mathbf{v} - \mathbf{v}^h\|_\Omega \leqslant C \left[\|\mathbf{v} - \Pi_h \mathbf{v}\|_\Omega + \Delta(\mathbf{v}^h) \right], \tag{2.22}$$

where $\Delta(\mathbf{v}^h)$ is the consistency term and C is a positive constant independent of h.

Remark 2.1. Error estimate (2.21) is suitable for straightforward analysis of different quadrature rules. Van Nooyen [9] has shown that for sufficiently smooth data and rectangular grids the use of a one-dimensional three-point quadrature rule in one direction and exact integration in the other yields an $O(h^4)$ error, while the FE method gives only an $O(h^2)$ error.

Error estimate (2.22) is suitable for analysis of elliptic problems that lack regularity. Since the consistency term depends only on discrete fluxes, its evaluation may be reduced to linear algebra analysis.

Proof. The theorem combines the well-known theoretical estimates for the L_2-norm of the flux (see e.g. [2,9]). Since the proof is very short, we shall provide it below.

Definition (2.20) and the mass balance equations imply that $\mathbf{r}^h \equiv \Pi_h \mathbf{v} - \mathbf{v}^h \in V_h$. Subtracting (2.2), with q and $\mathbf{w}$ replaced by q^h and $\mathbf{w}^h$, respectively, from (2.1), we get the Galerkin orthogonality property

$$
\begin{array}{lcl}
(K^{-1}\mathbf{r}^h, \mathbf{w}^h)_h - (p - p^h, \operatorname{div}\mathbf{w}^h) & = & (K^{-1}\Pi_h\mathbf{v}, \mathbf{w}^h)_h - (K^{-1}\mathbf{v}, \mathbf{w}^h), \\
(q^h, \operatorname{div}\mathbf{r}^h) & = & 0, \qquad \forall(\mathbf{w}^h, q^h) \in X_h \times Q_h.
\end{array}
$$

Here, we use (2.20) to obtain the second equation. Taking $\mathbf{w}^h = \mathbf{r}^h$ and using definition (2.19), we get

$$
(K^{-1}\mathbf{r}^h, \mathbf{r}^h)_h = (K^{-1}\Pi_h\mathbf{v}, \mathbf{r}^h)_h - (K^{-1}\mathbf{v}, \mathbf{r}^h).
$$

Now, the first assertion of the theorem follows from V_h-ellipticity assumption (2.14).

Denote by $\mathbf{w}^h = \Pi_h\mathbf{v}$ an element of X_h. The second assertion of the theorem follows from the Galerkin orthogonality property and the definition of V_h. We have

$$
\begin{array}{rcl}
(K^{-1}(\mathbf{w}^h - \mathbf{v}^h), \mathbf{u}^h) & = & (K^{-1}(\mathbf{w}^h - \mathbf{v}), \mathbf{u}^h) + (K^{-1}(\mathbf{v} - \mathbf{v}^h), \mathbf{u}^h) \\
& = & (K^{-1}(\mathbf{w}^h - \mathbf{v}), \mathbf{u}^h) + (p - p^h, \operatorname{div}\mathbf{u}^h) \\
& & -(K^{-1}\mathbf{v}^h, \mathbf{u}^h) + (K^{-1}\mathbf{v}^h, \mathbf{u}^h)_h \\
& = & (K^{-1}(\mathbf{w}^h - \mathbf{v}), \mathbf{u}^h) - (K^{-1}\mathbf{v}^h, \mathbf{u}^h) + (K^{-1}\mathbf{v}^h, \mathbf{u}^h)_h,
\end{array}
$$

for all $\mathbf{u}^h \in V_h$. Setting $\mathbf{u}^h = \mathbf{w}^h - \mathbf{v}^h \equiv \mathbf{r}^h \in V_h$ and using assumption (2.14) we get

$$
\|\mathbf{w}^h - \mathbf{v}^h\|_\Omega \leqslant C\left\{\|\mathbf{w}^h - \mathbf{v}\|_\Omega + \frac{|(K^{-1}\mathbf{v}^h, \mathbf{r}^h) - (K^{-1}\mathbf{v}^h, \mathbf{r}^h)_h|}{\|\mathbf{r}^h\|_{\operatorname{div},\,\Omega}}\right\}.
$$

Combining the last two formulae with the triangle inequality

$$
\|\mathbf{v} - \mathbf{v}^h\|_\Omega \leqslant \|\mathbf{v} - \mathbf{w}^h\|_\Omega + \|\mathbf{w}^h - \mathbf{v}^h\|_\Omega,
$$

we get error estimate (2.22). $\square$

In the end of this section we demonstrate one application of Theorem 2.1. Suppose that a pair of finite dimensional spaces Q_h and X_h is given by (2.7) and (2.8), respectively. The vector function η_e in (2.9) has zero normal components on all edges of the reference square and so does $J_e^{-1}\mathscr{J}_e\eta_e$. Recall that Q_h is the space of functions constant in each mesh element, and X_h is the space of vector functions with normal components continuous on each edge. Then the element-by-element application of the Green's formula shows that the inner product $(p^h, \operatorname{div}\mathbf{w}^h)$ does not depend on the particular choice for the discrete flux space (X_{1h} or X_{2h}). Therefore, the only difference between problems (2.2), (2.7), (2.8) and (2.2), (2.11), (2.8) consists in the way we compute the scalar product $(K^{-1}\mathbf{v}^h, \mathbf{w}^h)$. The quadrature rule given by the first problem will now be used as the quadrature rule for the second problem. We denote this quadrature rule by $(K^{-1}\mathbf{w}^h, \mathbf{u}^h)_h$, $(K^{-1}\mathbf{w}^h, \mathbf{u}^h)_h = (K^{-1}\mathbf{w}^h, \mathbf{u}^h)$ for all $\mathbf{w}^h, \mathbf{u}^h \in X_{1h}$. We show below that

$$(K^{-1}\mathbf{w}^h, \mathbf{u}^h)_h \approx (K^{-1}\mathbf{w}^h, \mathbf{u}^h), \qquad \forall \mathbf{w}^h, \mathbf{u}^h \in X_{2h},$$

and error estimates for problem (2.2), (2.7), (2.8) will follow from Theorem 2.1.

Lemma 2.1. *Let $\mathbf{w}^h, \mathbf{u}^h \in X_{2h}$ and the quadrature $(\cdot,\cdot)_h$ be as above. Then*

$$|(K^{-1}\mathbf{w}^h, \mathbf{u}^h) - (K^{-1}\mathbf{w}^h, \mathbf{u}^h)_h| \leqslant Ch\|\mathbf{w}^h\|_{\operatorname{div},\Omega}\|\mathbf{u}^h\|_{\operatorname{div},\Omega}, \tag{2.23}$$

where C is a positive constant independent of h.

Proof. Consider two arbitrary functions $\mathbf{w}^h, \mathbf{u}^h \in X_{2h}$ and estimate (2.23) element-by-element. To simplify notations we set $\mathbf{w}^h := \mathbf{w}^h|_e$ and $\mathbf{u}^h := \mathbf{u}^h|_e$ to be restrictions of the functions to element e. Denote by $\hat{\mathbf{w}}$, $\hat{\mathbf{u}}$, $\hat{\mathbf{w}}_i$, and $\hat{\mathbf{u}}_i$, $i = 1,2$, functions on reference element $\hat{e}$ related to functions $\mathbf{w}^h$, $\mathbf{u}^h$, $\mathbf{w}_i^h$, and $\mathbf{u}_i^h$, respectively, via Piola's transformation, e.g., $\mathbf{w}^h = \mathbf{F}_e^{-1} \circ J_e^{-1}\mathscr{J}_e\hat{\mathbf{w}}$. Also, set $\hat{\mathbf{w}} := (\hat{w}_{\hat{x}}, \hat{w}_{\hat{y}})^t$. Definition (2.10) implies that

$$\hat{\mathbf{w}} = \begin{bmatrix} \hat{w}_4 + \dfrac{\partial \hat{w}_{\hat{x}}}{\partial \hat{x}}\hat{x} \\[2ex] \hat{w}_1 + \dfrac{\partial \hat{w}_{\hat{y}}}{\partial \hat{y}}\hat{y} \end{bmatrix} + \eta_e \int_{\hat{e}} \hat{\operatorname{div}}\, \hat{\mathbf{w}}\, d\mathbf{r} \;\equiv\; \hat{\mathbf{w}}_1 + \hat{\mathbf{w}}_2$$

where $\hat{w}_1$ and $\hat{w}_4$ stand for the normal components of $\hat{\mathbf{w}}$ on edges l_1 and l_4, respectively. A similar formula holds for $\hat{\mathbf{u}}$, i.e., we may write $\hat{\mathbf{u}} = \hat{\mathbf{u}}_1 + \hat{\mathbf{u}}_2$.

Since $\hat{\mathbf{w}}_1, \hat{\mathbf{u}}_1 \in P_{10} \times P_{01}$, the quadrature rule is exact for inner product $(K^{-1}\mathbf{w}_1^h, \mathbf{u}_1^h)$. Moreover the definition of the quadrature rule implies that

$$(K^{-1}\mathbf{w}^h, \mathbf{u}^h)_h = (K^{-1}\mathbf{w}_1^h, \mathbf{u}_1^h).$$

One of the properties of Piola's transformation is that $\hat{\operatorname{div}}\, \hat{\mathbf{w}} = J_e \operatorname{div}\mathbf{w}^h$. Therefore,

$$\|\mathbf{w}_2^h\|_e \leqslant C|e|^{1/2}\, \|\eta_e\|_{\hat{e}}\, \|\operatorname{div}\mathbf{w}^h\|_e \leqslant Ch\|\operatorname{div}\mathbf{w}^h\|_e,$$

and

$$\|\mathbf{w}_1^h\|_e \leqslant \|\mathbf{w}^h\|_e + \|\mathbf{w}_2^h\|_e \leqslant \|\mathbf{w}^h\|_e + Ch\|\text{div}\,\mathbf{w}^h\|_e \leqslant C\|\mathbf{w}^h\|_{\text{div},\,e}.$$

Combining the last two inequalities with the regularity assumption for entries of tensor K, we get

$$|(K^{-1}\mathbf{w}_1^h, \mathbf{u}_2^h)_e| \leqslant C\|\mathbf{w}_1^h\|_e\|\mathbf{u}_2^h\|_e \leqslant Ch\|\mathbf{w}^h\|_{\text{div},\,e}\|\mathbf{u}^h\|_{\text{div},\,e}.$$

By symmetry, a similar estimate holds for $(K^{-1}\mathbf{w}_2^h, \mathbf{u}_1^h)_e$. The last term on the left hand side (2.23) is $(K^{-1}\mathbf{w}_2^h, \mathbf{w}_2^h)_e$ which is of order h^2. Summing elemental estimates and using the Cauchy-Schwartz inequality $\mathbf{a}^t\mathbf{b} \leqslant \|\mathbf{a}\|\|\mathbf{b}\|$, $\mathbf{a}, \mathbf{b} \in l_n$, we get the lemma assertion. □

With sufficient regularity the best approximation errors in Theorems 2.1 and 2.2 are of order h (see e.g. [13]). It follows from Lemma 2.1 that the error estimates for problem (2.2), (2.7), (2.8) are also of order h. Thus, we have the following standard error estimate for RT finite elements.

Theorem 2.3. *Under assumptions of Theorem* 2.1 *and Lemma* 2.1 *the error estimates*

$$\|\mathbf{v} - \mathbf{v}^h\|_{\text{div},\Omega} \leqslant C\,h\{\|\mathbf{v}\|_{1,\Omega} + \|\text{div}\,\mathbf{v}\|_{1,\Omega}\}$$

$$\|p - p^h\|_\Omega \leqslant C\,h\{\|\mathbf{v}\|_{1,\Omega} + \|p\|_{1,\Omega}\}$$

hold, with a positive constant C independent of h.

Proof. It is sufficient to show that the vector function $\mathbf{w}^h = \Pi_h\mathbf{v}$ satisfies $\|\mathbf{w}^h\|_{\text{div},\Omega} \leqslant C\|\mathbf{v}\|_{\text{div},\Omega}$. This estimate, as well as the theorem assertion, follows from the well known approximation results for the projector Π_h [2,11], Theorem 2.1, and Lemma 2.1. □

3. SUPPORT-OPERATOR DISCRETIZATION

In this section, we describe briefly the SO discretization (see, e.g., [6]) and prove that it provides at least the same error estimates as the lowest order RT finite element method. For the sake of simplicity, we describe the SO discretization for quadrilateral grids, since its generalization to arbitrary grids is straightforward.

We begin by introducing vector spaces of discrete functions together with inner products, which we will later relate to the finite element function spaces and their bilinear forms. Denote the vector space of cell-centered discrete scalar functions $q^d = (q_1, \ldots, q_{M_p})^t$ by Q_d, where M_p is the number of mesh cells. The scalar product on Q_d is given by

$$[p^d, q^d]_Q = \sum_{i=1}^{M_p} |e_i|\, p_i q_i, \qquad \forall p^d,\ q^d \in Q_d. \tag{3.1}$$

Obviously, vector space Q_d is isometric to finite element space Q_h from (2.8), i.e., for any $q^h \in Q_h$ there exists unique $q^d \in Q_d$, such that $q^h = \sum_{i=1}^{M_p} q_i \psi_i^h$ with piecewise constant basis functions $\psi_i^h \in Q_h$, $i = 1, \ldots, M_p$, and $(p^h, q^h) = [p^d, q^d]_Q$, for all $p^d, q^d \in Q_d$. We denote this isometry by $\mathscr{I}_Q$.

Denote the vector space of discrete edge-based vector functions $\mathbf{w}^d = (w_1, \ldots, w_{M_v})^t$ by X_d, where M_v is the number of mesh edges, and by $\mathbf{n}_i$, $i = 1, \ldots, M_v$ unit vectors orthogonal to mesh edges. Then w_i can be interpreted as the orthogonal projection of $\mathbf{w}^d$ on $\mathbf{n}_i$, i.e., $w_i = \mathbf{w}^d \cdot \mathbf{n}_i$. The scalar product on X_d is given by

$$[\mathbf{v}^d, \mathbf{w}^d]_X = \sum_{i=1}^{M_p} [\mathbf{v}^d, \mathbf{w}^d]_{X,i}, \tag{3.2}$$

where $[\mathbf{v}^d, \mathbf{w}^d]_{X,i}$ is an approximation of the scalar product of vector functions $K^{-1}\mathbf{v}^d$ and $\mathbf{w}^d$ on the i-th cell. One method for obtaining the formula for this scalar product is to use an isomorphism $\mathscr{I}_X$ between vector space X_d and finite element space X_{2h} from (2.11), since for any $\mathbf{w}^h \in X_{2h}$ there exists a unique $\mathbf{w}^d \in X_d$, such that $\mathbf{w}^h = \sum_{i=1}^{M_v} w_i \eta_i^h$, with the RT basis functions $\eta_i^h \in X_{2h}$, $i = 1, \ldots, M_v$. A difficulty in this approach is the necessity to integrate rational functions exactly over the unit square. An alternative approach was proposed in [6]. Note that the whole vector function can be recovered at four vertices of a quadrilateral from two orthogonal projections. Denoting the recovered vector at vertices by $\mathbf{v}_{i_j}^d$ and $\mathbf{w}_{i_j}^d$, $j = 1, \ldots, 4$, we define the approximate scalar product as

$$[\mathbf{v}^d, \mathbf{w}^d]_{X,i} = \frac{1}{2} \sum_{j=1}^{4} |T_{i_j}| K_{e_i}^{-1} \mathbf{v}_{i_j}^d \cdot \mathbf{w}_{i_j}^d, \tag{3.3}$$

where K_{e_i} is the value of K at the mass center of the quadrilateral, and $|T_{i_j}|$ is the area of the triangle with vertices $\mathbf{r}_{i_{j-1}}$, $\mathbf{r}_{i_j}$ and $\mathbf{r}_{i_{j+1}}$ (see Fig 1). For notational convenience, we set $\mathbf{r}_0 = \mathbf{r}_4$ and $\mathbf{r}_5 = \mathbf{r}_1$.

We now derive a discrete approximation to the divergence operator which we call the *prime operator*. Then we use the discrete divergence to derive an approximation to the gradient operator which we call the *derived operator*. We choose the prime operator to be the discrete divergence $\mathrm{DIV} : X_d \to Q_d$, which follows naturally from the Gauss divergence theorem as

$$(\mathrm{DIV}\mathbf{w}^d)_i = \frac{1}{|e_i|} \left(w_{i_2}|l_2| - w_{i_4}|l_4| + w_{i_3}|l_3| - w_{i_1}|l_1| \right), \qquad i = 1, \ldots, M_p. \tag{3.4}$$

Consequently, the derived operator is the discrete gradient GRAD. It is defined by $\mathrm{GRAD} = -\mathrm{DIV}^*$, where the adjoint operator is taken with respect to scalar products (3.1) and (3.2), (3.3), i.e.,

$$[\mathrm{DIV}\mathbf{w}^d, q^d]_Q = -[\mathbf{w}^d, \mathrm{DIV}^* q^d]_X, \qquad \forall \mathbf{w}^d \in X_d, \quad \forall q^d \in Q_d,$$

which is the discrete Green's formula. To derive the explicit formula for GRAD, we consider an auxiliary scalar product $< \cdot, \cdot >$ and relate it to scalar products (3.1) and (3.2). Denote by $< \cdot, \cdot >$ the usual vector dot product. Then

$$[p^d, q^d]_Q = < \mathscr{D} p^d, q^d >, \qquad \text{and} \qquad [\mathbf{v}^d, \mathbf{w}^d]_X = < \mathscr{M} \mathbf{v}^d, \mathbf{w}^d >,$$

where $\mathscr{D}$ is a diagonal matrix, $\mathscr{D} = \operatorname{diag}\{|e_1|, \ldots, |e_{M_p}|\}$, and $\mathscr{M}$ is a sparse symmetric mass matrix corresponding to a 5-point stencil. Restricted to a cell, this stencil connects edge-based unknowns if and only if the corresponding edges have a common point. Combining the last two formulae, we get

$$\begin{aligned} [\mathbf{w}^d, \mathrm{DIV}^* q^d]_X &= \; < \mathbf{w}^d, \mathscr{M}\, \mathrm{DIV}^* q^d > = \; -[\mathrm{DIV}\mathbf{w}^d, q^d]_Q \\ &= \; - < \mathbf{w}^d, \mathrm{DIV}^t\, \mathscr{D}\, q^d >, \qquad \forall \mathbf{w}^d \in X_d, \quad \forall q^d \in Q_d, \end{aligned}$$

where DIV^t is the adjoint of DIV with respect to the auxiliary scalar product. Therefore,

$$\mathrm{GRAD} = \mathscr{M}^{-1}\, \mathrm{DIV}^t\, \mathscr{D}. \tag{3.5}$$

The finite difference methods approximating the first-order system (1.1) may be summarized as follows

$$\mathbf{v}^d = \mathrm{GRAD}\, p^d, \qquad \mathrm{DIV}\, \mathbf{v}^d = f^d, \tag{3.6}$$

where $f^d = (f_1, \ldots, f_{M_p})^t$ and entry f_i is the integral average of f over cell e_i.

The basic tool for accuracy analysis of the discrete solution $(\mathbf{v}^d, p^d) \in X^d \times Q^d$ is based on Theorems 2.1 – 2.3. We use the isometry $\mathscr{I}_Q$ and isomorphism $\mathscr{I}_X$ to establish a relationship between (2.2) and (3.6). Multiplying the first equation in (3.6) by $\mathscr{M}\mathbf{w}^d$ and the second one by $\mathscr{D} q^d$, we get

$$\begin{aligned} &[\mathbf{v}^d, \mathbf{w}^d]_X - [p^d, \mathrm{DIV}\, \mathbf{w}^d]_Q \;=\; 0, \\ &[q^d, \mathrm{DIV}\, \mathbf{v}^d]_Q \qquad\qquad\qquad\;\; = [f^d, q^d]_Q, \qquad \forall (\mathbf{w}^d, q^d) \in X_d \times Q_d. \end{aligned} \tag{3.7}$$

Let $q^h = \mathscr{I}_Q(q^d)$ and $\mathbf{w}^h = \mathscr{I}_X(\mathbf{w}^d)$. The equivalence of (2.12) and (3.4) gives that

$$[p^d, \mathrm{DIV}\, \mathbf{w}^d]_Q = (p^h, \operatorname{div} \mathbf{w}^h), \qquad \forall \mathbf{w}^d \in X_d, \quad \forall q^d \in Q_d.$$

The definition of f^d implies that

$$[f^d, q^d]_Q = (f^h, q^h) = (f, q^h).$$

Finally, by introducing the quadrature rule

$$(K^{-1}\mathbf{v}^h, \mathbf{w}^h)_h \equiv [\mathbf{v}^d, \mathbf{w}^d]_X, \qquad \forall \mathbf{v}^d, \mathbf{w}^d \in X_d, \tag{3.8}$$

we reduce problem (3.7) to finite element problem (2.2). Therefore Theorems 2.1 and 2.2 can be used to derive error estimates for problem (3.6).

The SO discretization for the case of triangular grids is formulated similarly. Its equivalence with finite element problem (2.2), (2.7), (2.8) can also be established. The quadrature rule in this case is given by (3.2) with elemental scalar products

$$[\mathbf{v}^d, \mathbf{w}^d]_{X,i} = \frac{1}{3}|e_i| \sum_{j=1}^{3} K_{e_i}^{-1} \mathbf{v}_{i_j}^d \cdot \mathbf{w}_{i_j}^d, \tag{3.9}$$

where K_{e_i} is the value of K at the mass center of e_i.

3.1. Error estimates for the SO discretization

As in the previous sections, we assume that the entries of tensor K are sufficiently smooth, e.g., in $C^1(\Omega)$, $\mathbf{v} \in (H^1(\Omega))^2$, and $\operatorname{div} \mathbf{v} \in H^1(\Omega)$. Our main results are captured in Lemmas 3.1 and 3.2, and in Theorem 3.1.

We begin by noting that scalar product (3.8) is continuous. Let us check that it satisfies V_h-ellipticity condition (2.14). Recall that V_h is the space of divergent-free functions, i.e. $\operatorname{div} \mathbf{w}^h = 0$ for $\mathbf{w}^h \in V_h$. The definition of the quadrature rule implies that $(\mathbf{w}^h, \mathbf{w}^h)_h$ generates a norm on X_h. Therefore

$$(K^{-1}\mathbf{w}^h, \mathbf{w}^h)_h \geqslant \|K\|_{0,\infty}^{-1} (\mathbf{w}^h, \mathbf{w}^h)_h \geqslant C \|\mathbf{w}^h\|_\Omega^2 = C \|\mathbf{w}^h\|_{\operatorname{div},\Omega}^2, \qquad \forall \mathbf{w}^h \in V_h.$$

Lemma 3.1. *Suppose $\mathscr{T}_h$ is a shape regular triangulation of $\bar{\Omega}$. Denote functions in the discrete flux space X_h defined in* (2.3) *by $\mathbf{w}^h$ and $\mathbf{u}^h$. If the quadrature rule is given by* (3.2)*,* (3.9) *and* (3.8)*, then*

$$|(K^{-1}\mathbf{w}^h, \mathbf{u}^h) - (K^{-1}\mathbf{w}^h, \mathbf{u}^h)_h| \leqslant Ch\|\mathbf{w}^h\|_{\operatorname{div},\Omega}\|\mathbf{u}^h\|_{\operatorname{div},\Omega}, \tag{3.10}$$

where C is a positive constant independent of h.

Proof. The proof consists of two steps. First, we show that scalar product $(K^{-1}\mathbf{w}^h, \mathbf{u}^h)$ can be approximated by scalar product $(K_h^{-1}\mathbf{w}^h, \mathbf{u}^h)$ where K_h is a piecewise constant tensor with the constant cell values K_e, $e \in \mathscr{T}_h$ introduced above. Second, we evaluate $|(K_h^{-1}\mathbf{w}^h, \mathbf{u}^h) - (K_h^{-1}\mathbf{w}^h, \mathbf{u}^h)_h|$. The lemma assertion will follow from the triangle inequality.

For $e \in \mathscr{T}_h$, we have

$$\begin{aligned} \left| \int_e (K^{-1} - K_h^{-1}) \mathbf{w}^h \cdot \mathbf{u}^h \, d\mathbf{r} \right| &\leqslant \|K^{-1} - K_e^{-1}\|_{0,\infty,e} \|\mathbf{w}^h\|_e \|\mathbf{u}^h\|_e \\ &\leqslant Ch \|K^{-1}\|_{1,\infty,e} \|\mathbf{w}^h\|_e \|\mathbf{u}^h\|_e. \end{aligned}$$

Summing up the local estimates and using the regularity of K, we get

$$|(K^{-1}\mathbf{w}^h, \mathbf{u}^h) - (K_h^{-1}\mathbf{w}^h, \mathbf{u}^h)| \leqslant Ch \|\mathbf{w}^h\|_\Omega \|\mathbf{u}^h\|_\Omega. \tag{3.11}$$

The key point for the second step is a special decomposition of discrete vector functions. Setting $\mathbf{w}^h := \mathbf{w}^h|_e$, we can verify that

$$\mathbf{w}^h(\mathbf{r}) = \mathbf{w}^h(\mathbf{r}_0) + \frac{1}{2}(\operatorname{div}\mathbf{w}^h)(\mathbf{r}-\mathbf{r}_0), \qquad \forall \mathbf{r}_0 \in e. \tag{3.12}$$

Denote by $\sigma_e(\mathbf{w}^h, \mathbf{u}^h) \equiv (K_h^{-1}\mathbf{w}^h, \mathbf{u}^h) - (K_h^{-1}\mathbf{w}^h, \mathbf{u}^h)_h$ the elemental error. Since the quadrature rule (3.2), (3.9) is exact for constant functions, we get

$$\begin{aligned} |\sigma_e(\mathbf{w}^h, \mathbf{u}^h)| &\leqslant \tfrac{1}{2}|\sigma_e(\mathbf{w}^h(\mathbf{r}_0), (\operatorname{div}\mathbf{u}^h)(\mathbf{r}-\mathbf{r}_0))| \\ &+ \tfrac{1}{2}|\sigma_e((\operatorname{div}\mathbf{w}^h)(\mathbf{r}-\mathbf{r}_0), \mathbf{u}^h(\mathbf{r}_0))| \\ &+ \tfrac{1}{4}|\sigma_e((\operatorname{div}\mathbf{w}^h)(\mathbf{r}-\mathbf{r}_0), (\operatorname{div}\mathbf{u}^h)(\mathbf{r}-\mathbf{r}_0))|. \end{aligned}$$

Set $\mathbf{r}_0 = (x_0, y_0)^t$ to be the mass center of triangle e and define $\mathbf{r} := (x, y)^t$. We now show that the first two terms are zero. Because $K_e^{-1}\mathbf{w}^h(\mathbf{r}_0) \equiv \mathbf{a} = (a, b)^t$ is a constant vector function, we get

$$\int_e K_e^{-1}\mathbf{w}^h(\mathbf{r}_0)\cdot(\mathbf{r}-\mathbf{r}_0)\,d\mathbf{r} = \int_e [a(x-x_0) + b(y-y_0)]\,\mathrm{d}\mathbf{r} = 0.$$

We set $\mathbf{r}_i := (x_i, y_i)$, $i = 1,2,3$, and denote by $\mathbf{r}_i$ the triangle vertices. Noting that $\operatorname{div}\mathbf{u}^h$ is constant in e, this yields

$$(\mathbf{a}, (\mathbf{r}-\mathbf{r}_0))_h = \frac{|e|}{3}\sum_{j=1}^{3}\mathbf{a}\cdot(\mathbf{r}_j-\mathbf{r}_0) = \frac{|e|}{3}\sum_{j=1}^{3}[a(x_j-x_0)+b(y_j-y_0)] = 0.$$

Therefore the first term is zero. Symmetry between the first two terms implies that the second term is also zero. Finally,

$$\begin{aligned} |\sigma_e(\mathbf{w}^h, \mathbf{u}^h)| &= \tfrac{1}{4}|(\operatorname{div}\mathbf{w}^h)(\operatorname{div}\mathbf{u}^h)\sigma_e(\mathbf{r}-\mathbf{r}_0, \mathbf{r}-\mathbf{r}_0)| \\ &\leqslant Ch^2\|\operatorname{div}\mathbf{w}^h\|_{\operatorname{div},e}\|\operatorname{div}\mathbf{u}^h\|_{\operatorname{div},e}. \end{aligned} \tag{3.13}$$

Summing up elemental estimates (3.13) and combining the result with (3.11), we obtain the lemma assertion. □

In the case of quadrilateral grids, the analysis of the consistency term is more complicated. It involves inverse estimates which impose additional restrictions on the shape regularity of these grids. The theoretical estimates will be proved for shape regular quasi-uniform quadrilateral partitions (see, e.g. [1]).

Lemma 3.2. *Suppose $\mathscr{T}_h$ is a shape regular quasi-uniform quadrilateral partition of $\bar{\Omega}$. Denote functions from the discrete flux space X_{2h} defined in* (2.11) *by $\mathbf{w}^h$ and $\mathbf{u}^h$. If the quadrature rule is given by* (3.2), (3.3) *and* (3.8), *then*

$$|(K^{-1}\mathbf{w}^h, \mathbf{u}^h) - (K^{-1}\mathbf{w}^h, \mathbf{u}^h)_h| \leqslant Ch\,\|\mathbf{w}^h\|_{1,\Omega}\,\|\mathbf{u}^h\|_{\operatorname{div},\Omega}, \tag{3.14}$$

where C is a positive constant independent of h.

Proof. The proof consists of three steps. The first step is a repetition of the first step in the proof of Lemma 3.1 for quadrilateral e. It results in the estimate

$$|(K^{-1}\mathbf{w}^h, \mathbf{u}^h) - (K_h^{-1}\mathbf{w}^h, \mathbf{u}^h)| \leqslant Ch\,\|\mathbf{w}^h\|_\Omega\,\|\mathbf{u}^h\|_\Omega. \tag{3.15}$$

The second step is an application of Lemma 2.1, which states that the scalar product of the modified RT finite elements may be approximated by the scalar product of the standard RT finite elements. Denoting the latter by $(\cdot,\cdot)_{RT}$, we get

$$|(K_h^{-1}\mathbf{w}^h, \mathbf{u}^h) - (K_h^{-1}\mathbf{w}^h, \mathbf{u}^h)_{RT}| \leqslant Ch\,\|\mathbf{w}^h\|_{\mathrm{div},\Omega}\,\|\mathbf{u}^h\|_{\mathrm{div},\Omega}. \tag{3.16}$$

The key point for the third step is based on a special decomposition of discrete vector functions. Setting $\mathbf{w}^h := \mathbf{w}^h|_e$ we can write

$$\mathbf{w}^h = \mathbf{w}^h(\mathbf{r}_0) + \mathbf{w}_1^h, \qquad \mathbf{w}_1^h = \mathbf{F}_e^{-1} \circ \frac{1}{J_e}\mathscr{J}_e\hat{\mathbf{w}}_1,$$

where $\mathbf{r}_0 \in e$ and $\hat{\mathbf{w}}_1$ is a linear function on the reference element $\hat{e}$. The definition of RT finite elements implies that

$$\hat{\mathbf{w}}_1 = \begin{bmatrix} w_{1x}(\hat{x}-\hat{x}_0) \\ w_{1y}(\hat{y}-\hat{y}_0) \end{bmatrix},$$

with some constants w_{1x} and w_{1y}. Similar formulae hold for $\mathbf{u}^h$, i.e., $\mathbf{u}^h = \mathbf{u}^h(\mathbf{r}_0) + \mathbf{u}_1^h$. Denote by

$$\sigma_e(\mathbf{w}^h, \mathbf{u}^h) \equiv (K_h^{-1}\mathbf{w}^h, \mathbf{u}^h)_{RT} - (K_h^{-1}\mathbf{w}^h, \mathbf{u}^h)_h$$

the elemental error. Since quadrature rule (3.2), (3.3) is exact for constant functions, we get

$$|\sigma_e(\mathbf{w}^h, \mathbf{u}^h)| \leqslant |\sigma_e(\mathbf{w}^h(\mathbf{r}_0), \mathbf{u}_1^h)| + |\sigma_e(\mathbf{w}_1^h, \mathbf{u}^h(\mathbf{r}_0))| + |\sigma_e(\mathbf{w}_1^h, \mathbf{u}_1^h)|.$$

We shall show that the first two terms are zero if $\mathbf{r}_0 = (\mathbf{r}_1+\mathbf{r}_2+\mathbf{r}_3+\mathbf{r}_4)/4$. This implies that $\hat{\mathbf{r}}_0 := (\hat{x}_0, \hat{y}_0)^t = (1/2, 1/2)^t$. Denote by $\mathbf{a} = (a, b)^t$ a constant vector function given by $\mathbf{a} = K_e^{-1}\mathbf{w}^h(\mathbf{r}_0)$. Then the exact value of $(\mathbf{a}, \mathbf{u}_1^h)$ is zero. Since $\hat{x}-\hat{x}_0$ and $\hat{y}-\hat{y}_0$ both are symmetric about the points $\hat{x}_0$ and $\hat{y}_0$, respectively, we have

$$\begin{aligned}\int_e \mathbf{a}\cdot\mathbf{u}_1^h \,\mathrm{d}\mathbf{r} &= \int_e J_e^{-1}\mathbf{a}\cdot\mathscr{J}_e\mathbf{u}_1^h\,\mathrm{d}\mathbf{r} \\ &= \int_{\hat{e}} u_{1x}(\hat{x}-\hat{x}_0)\,\mathbf{a}\cdot\mathbf{j}_1(\hat{y})\,\mathrm{d}\hat{\mathbf{r}} + \int_{\hat{e}} u_{1y}(\hat{y}-\hat{y}_0)\,\mathbf{a}\cdot\mathbf{j}_2(\hat{x})\,\mathrm{d}\hat{\mathbf{r}} = 0\end{aligned}$$

where $\mathbf{j}_1(\hat{y})$ and $\mathbf{j}_2(\hat{x})$ are the first and the second columns of Jacobian $\mathscr{J}_e$, respectively. The quadrature rule (3.2), (3.3) yields

$$(\mathbf{a}, \mathbf{u}_1^h)_h = \frac{1}{2}\sum_{j=1}^{4}\frac{|T_j|}{J_e(\hat{\mathbf{r}}_j)}\,\mathbf{a}\cdot\mathscr{J}_e(\hat{\mathbf{r}}_j)\hat{\mathbf{u}}_1(\hat{\mathbf{r}}_j),$$

where $\hat{\mathbf{r}}_j$, $j = 1,2,3,4$, are vertices of the reference square $\hat{e}$ and $|T_j|$ is the area of the triangle with vertices $\mathbf{r}_{j-1}$, $\mathbf{r}_j$ and $\mathbf{r}_{j+1}$ (see Fig. 1). It follows from (2.6) that $J_e(\hat{\mathbf{r}}_j) = 2|T_j|$. Straightforward computation of $\mathscr{J}_e(\hat{\mathbf{r}}_j)$ result in

$$\begin{aligned}\sum_{j=1}^{4} \mathscr{J}_e(\hat{\mathbf{r}}_j)\hat{\mathbf{u}}_1(\hat{\mathbf{r}}_j) \;=\; & -\hat{x}_0\, u_{1x}\mathbf{r}_{21} && - \;\; \hat{y}_0\, u_{1y}\mathbf{r}_{41} \\ & +(1-\hat{x}_0)u_{1x}\mathbf{r}_{21} && - \;\; \hat{y}_0\, u_{1y}\mathbf{r}_{32} \\ & +(1-\hat{x}_0)u_{1x}\mathbf{r}_{34} && + \;\; (1-\hat{y}_0)u_{1y}\mathbf{r}_{32} \\ & + -\hat{x}_0\, u_{1x}\mathbf{r}_{34} && + \;\; (1-\hat{y}_0)u_{1y}\mathbf{r}_{41} \\ =\; & \mathbf{0}, \end{aligned}$$

where $\mathbf{r}_{ij} = \mathbf{r}_i - \mathbf{r}_j$. Thus, $\sigma_e(\mathbf{w}^h(\mathbf{r}_0), \mathbf{u}_1^h) = 0$, and by symmetry, $\sigma_e(\mathbf{w}_1^h, \mathbf{u}^h(\mathbf{r}_0)) = 0$. In order to estimate the third term, we recall that $\mathbf{w}_1^h(\mathbf{r}_0) = \mathbf{u}_1^h(\mathbf{r}_0) = \mathbf{0}$. Therefore a Poincaré-Friedrichs type inequality holds, which implies that

$$\|\mathbf{w}_1^h\|_e \leqslant Ch\,|\mathbf{w}_1^h|_{1,e} = Ch\,|\mathbf{w}^h|_{1,e}, \qquad \text{and} \qquad \|\mathbf{u}_1^h\|_e \leqslant Ch\,|\mathbf{u}^h|_{1,e}.$$

Using the regularity of K and the inverse estimate [1], we obtain

$$|\sigma_e(\mathbf{w}^h, \mathbf{u}^h)| \leqslant Ch^2|\mathbf{w}^h|_{1,e}|\mathbf{u}^h|_{1,e} \leqslant Ch\,|\mathbf{w}^h|_{1,e}\|\mathbf{u}^h\|_e.$$

Summing up the elemental estimates and combining the result with (3.15) and (3.16), we get the lemma assertion. □

With sufficient regularity, the best approximation errors in Theorems 2.1 and 2.2 are of order h (see e.g. [13] or Theorem 2.3). If follows from Lemmas 3.1 and 3.2 that the error estimates for problem (3.6) are also of order h. In fact we have the following result.

Theorem 3.1. *Suppose $\mathscr{T}_h$ is either a shape regular triangular or a quasi-uniform quadrilateral partitioning of $\bar{\Omega}$ and input data are sufficiently smooth. Denote the solution of the support-operators discretization* (3.6) *by $(\mathbf{v}^d, p^d)$, and set $\mathbf{v}^h = \mathscr{I}_X(\mathbf{v}^d)$ and $p^h = \mathscr{I}_Q(p^d)$. Then the following error bounds hold*

$$\begin{aligned} &\|\mathbf{v} - \mathbf{v}^h\|_{\mathrm{div},\Omega} \leqslant C\,h\,\{\,\|\mathbf{v}\|_1 + \|\mathrm{div}\,\mathbf{v}\|_1\,\}\,, \\ &\|p - p^h\|_{\Omega} \leqslant C\,h\,\{\,\|p\|_1 + \|\mathbf{v}\|_1\,\}\,, \end{aligned}$$

with a positive constant C independent of h.

Proof. In the case of triangular grids, it is sufficient to show that the vector function $\mathbf{w}^h = \Pi_h\mathbf{v}$ satisfies $\|\mathbf{w}^h\|_{\mathrm{div},\Omega} \leqslant C\|\mathbf{v}\|_{\mathrm{div},\Omega}$. In the case of quadrilateral grids, it is sufficient to show that $\|\mathbf{w}^h\|_{1,\Omega} \leqslant C\|\mathbf{v}\|_{1,\Omega}$. These estimates, as well as the theorem assertion, follow from the well known approximation results for the projector Π_h [2,11], Theorem 2.1 and Lemmas 3.1 and 3.2. □

4. NUMERICAL EXPERIMENTS

In this section, we present results of numerical experiments to verify our theoretical error estimates. We compare the convergence rate for both the RT finite element and SO discretizations on a sequence of refined quadrilateral grids. In addition, we shall show that to achieve a given error, quadrilateral grids require less unknowns than triangular grids.

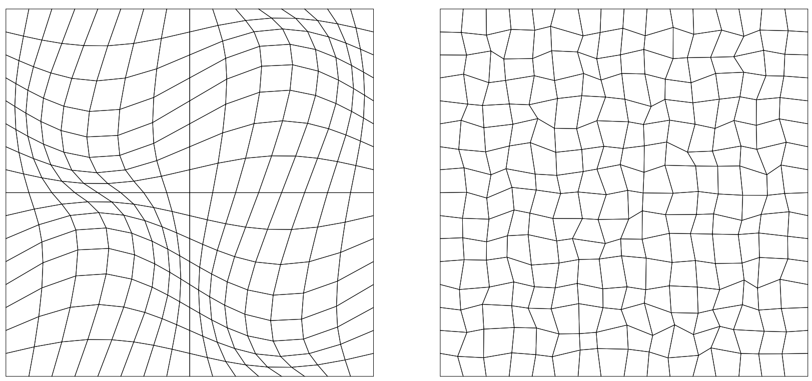

Figure 2. Example of 16x16 smooth and random shape regular grids.

Two types of grids were used in our experiments: smooth and random (see Figure 2). The smooth grid is constructed from a rectangular grid via mapping

$$x(\xi,\eta) = \xi + 0.1\,\sin(2\pi\eta)\,\sin(2\pi\xi), \qquad y(\xi,\eta) = \eta + 0.1\,\sin(2\pi\eta)\,\sin(2\pi\xi),$$

where $0 < \eta, \xi < 1$. The random grid is constructed by random distortions of the mesh node positions. The maximal value of the distortion is half of the mesh cell size (50%) which guarantees that the final grid will consist of convex quadrilaterals.

Let us assume that $K = I$ and equation (1.1) have the exact solution

$$p(x,y) = (|x-0.5|^{\alpha} - 0.5^{\alpha})\,(|y-0.5|^{\alpha} - 0.5^{\alpha}), \qquad 0 \leqslant x, y \leqslant 1,$$

where $\alpha = 2.6$. It is easy to check that $\operatorname{div} \mathbf{v} = \Delta p \in H^1(\Omega)$ and $\mathbf{v} \in (H^1(\Omega))^2$.

Denote the errors we computed in our experiments by $\varepsilon_p = \|p - p^h\|_{\Omega}$ and $\varepsilon_{\mathbf{v}} = \|\mathbf{v} - \mathbf{v}^h\|_{\mathrm{div},\Omega}$. For the sake of simplicity, we computed the errors approximately by splitting quadrilaterals into triangles and applying a 5th order quadrature for each triangle. The result of numerical experiments are shown in Tables 1 and 2. Note that, instead of constructing a sequence of embedded random grids, we averaged computed errors over 10 random grids.

It is easy to observe the convergence rate of order h for both methods. Asymptotically, the methods give the same approximation errors. This means that the consistency error is much smaller than the approximation error. In fact, Lemma 3.1 states

Table 1.
Convergence rate on a sequence of smooth grids.

h^{-1}	modified RT FE		SO FD	
	ε_p	$\varepsilon_{\mathbf{v}}$	ε_p	$\varepsilon_{\mathbf{v}}$
16	1.58e-3	2.34e-2	1.61e-3	2.35e-2
32	7.95e-4	1.22e-2	7.99e-4	1.22e-2
64	3.98e-4	6.29e-3	3.99e-4	6.29e-3
128	1.99e-4	3.22e-3	1.99e-4	3.22e-3
256	9.97e-5	1.64e-3	9.97e-5	1.64e-3
512	4.98e-5	8.32e-4	4.98e-5	8.32e-4

Table 2.
Convergence rate on a sequence of random grids.

h^{-1}	modified RT FE		SO FD	
	ε_p	$\varepsilon_{\mathbf{v}}$	ε_p	$\varepsilon_{\mathbf{v}}$
16	1.42e-3	2.24e-2	1.43e-3	2.25e-2
32	7.15e-4	1.17e-2	7.18e-4	1.17e-2
64	3.59e-4	5.96e-3	3.59e-4	5.98e-3
128	1.80e-4	3.06e-3	1.80e-4	3.07e-3
256	9.00e-5	1.56e-3	9.00e-5	1.56e-3
512	4.50e-5	7.93e-4	4.50e-5	7.93e-4

that the consistency error for triangular partitions is of order h^2, when $K = I$. The numerical results show that a similar conclusion may be also drawn for quadrilateral partitions.

Surprisingly, the convergence rate is slightly better on the sequence of random grids. Nevertheless, the gain is only 10% for ε_p and about 5% for $\varepsilon_{\mathbf{v}}$. Let us analyze how the convergence rate depends on the grid distortion. The results of numerical experiments for the SO discretizations and three values of the distortion factor are shown in Table 3. Similar results for the maximal permissible distortion of 50% are shown in the last two columns of Table 2. A very mild deterioration of the error is observed, when the distortion factor is changed from 0% to 50%.

In our last experiment, we compared the errors for triangular and quadrilateral grids. The triangular grids were obtained by splitting each quadrilateral into two triangles. We studied three splitting algorithms. First, every quadrilateral was split by the diagonal connecting the upper left corner with the lower right corner. Second, two neighboring quadrilaterals were split by opposite diagonals. Third, the shortest diagonal for each quadrilateral was used to subdivied a given quadrilateral. For the smooth grid, the best approximation results were achieved in the third case. The result of numerical experiments for the SO discretization are shown in Table 4.

The triangulation of a quadrilateral grid results in a bigger algebraic problem: We get approximately 1.6 times more unknowns. A quadrilateral grid with the same number of unknowns will correspond to a mesh size of $0.77h$. Since the convergence rate is linear in h, we get a smaller error $\varepsilon_{\mathbf{v}}$ for such a grid. Thus, for a given error,

Table 3.
Convergence rate for different distortion factors.

h^{-1}	Distortion factor					
	0 %		20 %		40 %	
	ε_p	$\varepsilon_{\mathbf{v}}$	ε_p	$\varepsilon_{\mathbf{v}}$	ε_p	$\varepsilon_{\mathbf{v}}$
16	1.38e-3	2.17e-2	1.39e-3	2.19e-2	1.42e-3	2.21e-2
32	6.87e-4	1.12e-2	6.92e-4	1.13e-2	7.07e-4	1.16e-2
64	3.43e-4	5.75e-3	3.45e-4	5.81e-3	3.53e-4	5.93e-3
128	1.71e-4	2.93e-3	1.73e-4	2.96e-3	1.77e-4	3.03e-3
256	8.57e-5	1.49e-3	8.64e-5	1.51e-3	8.84e-5	1.54e-3
512	4.28e-5	7.57e-4	4.32e-5	7.65e-4	4.42e-5	7.82e-4

Table 4.
Convergence rate on triangular and quadrilateral grids.

h^{-1}	Smooth triangular grid				Smooth quadrilateral grid			
	ε_p	$\varepsilon_{\mathbf{v}}$	$\dim Q_d$	$\dim X_d$	ε_p	$\varepsilon_{\mathbf{v}}$	$\dim Q_d$	$\dim X_d$
16	1.25e-3	1.90e-2	512	800	1.61e-3	2.35e-2	256	544
32	6.20e-4	9.86e-2	2048	3136	7.99e-4	1.22e-2	1024	2112
64	3.09e-4	5.07e-3	8192	12416	3.99e-4	6.29e-3	4096	8320
128	1.54e-4	2.60e-3	32768	49408	1.99e-4	3.22e-3	16384	33024
256	7.72e-5	1.32e-3	131072	197120	9.97e-5	1.64e-3	65536	131584
512	3.86e-5	6.72e-4	524288	787456	4.98e-5	8.32e-4	262144	525312

quadrilateral grids require less unknowns than triangular grids.

5. CONCLUSION

In this paper, we rigorously establish convergence of the mimetic discretization of the linear diffusion equation based on the support operator methodology. This is achieved by deriving error estimates for the SO discretization using error estimates for the modified RT finite element method. Specifically, we proved that the SO discretization is as accurate as the lowest order modified RT finite element method. We observed in numerical experiments that, asymptotically, both methods result in the same errors. Our work provides analytic evidence consistent with the successful application of the SO discretization to linear diffusion problems.

We note that the approach presented in this paper can be used to derive additional error estimates. For example, Theorem 2.2 can be used to obtain L_2 error estimates for the flux variable. Further, a standard technique for deriving superconvergence error estimates can be used to prove similar results for the SO method. However, we shall leave this for a future paper.

Acknowledgments. The authors thank Prof. Yuri Kuznetsov, University of Houston, for showing some relationships between the SO and RT finite element methods and for many other fruitful comments. We also thank Jim Morel, Los Alamos National Laboratory, for fruitful discussions.

REFERENCES

1. D. Braess, *Finite Elements : Theory, Fast Solvers, and Applications in Solid Mechanics.* Cambridge University Press, Cambridge, U.K., New York, 1997.
2. F. Brezzi and M. Fortin, *Mixed and Hybrid Finite Element Methods.* Springer Verlag, Berlin, 1991.
3. J. Campbell and M. Shashkov, A tensor artificial viscosity using a mimetic finite difference algorithm. *Journal of Computational Physics.* (2001) **172**, 739–765.
4. P. G. Ciarlet, Basic Error Estimates for Elliptic Problems. In: *Handbook of Numerical Analysis, vol II: Finite Element Methods* (Eds. P.G.Ciarlet and J.L.Lions). Elsevier/North Holland, Amsterdam, 1991, pp. 17–352.
5. J. Hyman and M. Shashkov, Mimetic discretizations for Maxwell's equations and the equations of magnetic diffusion. *Progress in Electromagnetic Research.* (2001) **32**, 89–121.
6. J. Hyman, M. Shashkov, and S. Steinberg, The numerical solution of diffusion problems in strongly heterogeneous non-isotropic materials. *Journal of Computational Physics.* (1997) **132**, 130–148.
7. J. Hyman, M. Shashkov, and S. Steinberg, Inner products for discrete vector fields and accuracy of mimetic difference methods. *Los Alamos National Laboratory.* Report LA-UR-99-6181, January, 2000.
8. J. E. Morel, R. M. Roberts, and M. J. Shashkov, A local support-operators diffusion discretization scheme. *Journal of Computational Physics.* (1998) **144**, 17–51.
9. R. R. P. van Nooyen, An improved accuracy version of the mixed finite-element method for a

second-order elliptic equation. *Journal of Computational and Applied Mathematics.* (1993) **47**, 11–33.

10. P. A. Raviart and J. M. Thomas, A mixed finite element method for second order elliptic problems. In: *Mathematical Aspects of the Finite Element Method* (Eds. I.Galligani and E.Magenes). Springer-Verlag, Berlin-Heilderberg-New York, 1977, pp. 292–315.
11. J. E. Roberts and J. M. Thomas, Mixed and Hybrid Methods. In: *Handbook of Numerical Analysis, vol II: Finite Element Methods* (Eds. P.G.Ciarlet and J.L.Lions). Elsevier/North Holland, Amsterdam, 1991, pp. 523–640.
12. M. Shashkov and S. Steinberg, Solving diffusion equations with rough coefficients in rough grids. *Journal of Computational Physics.* (1996) **129**, 383–405.
13. J. Shen, Mixed finite element methods on distorted rectangular grids. Institute for Scientific Computation, Texas A&M University, Report ISC-94-13-MATH, July, 1994.
14. J. M. Thomas, *Sur l'analyse numérique des méthods d'éléments finis hybrides et mixtes*, PhD thesis, Université Pierre et Marie Curie, Paris, 1977.
15. J. Wang and T. Mathew, Mixed finite element methods over quadritaterals. In: *Third International Conference on Advances in Numerical Methods adn Applications* (Eds. I.T.Dimov, B.Sedov, and P.Vassilevski). World Scientific, 1994, pp. 203–214.